Paper 057

Large scale evaporating liquid cascades – an experimental and computational study

Coldrick, S., Atkinson, G.T., Gant, S.E.

Health and Safety Laboratory, Harpur Hill, Buxton, Derbyshire, SK17 9JN

Abstract

The Buncefield incident demonstrated that large flammable vapour clouds can be generated by liquid cascades resulting from overfilling bulk storage tanks. The vapour cloud produced in that incident was observed to be relatively deep and slow moving, and was therefore able to spread under low wind speed conditions across a wide area without significant dilution before it ignited. Recently, a series of large scale experiments have been undertaken at HSL to further our understanding of vapour cloud generation. In conjunction with the experiments, Computational Fluid Dynamics (CFD) simulations have been carried out. This paper presents some preliminary results from the ongoing series of experiments and simulations.

The experimental facility consisted of a vertical wall that replicated a section of a typical hydrocarbon storage tank with a wind girder. A spill system at the top of the tank produced liquid cascades with flowrates representative of overfilling incidents. Measurements of the temperature of the resulting vapour current were made using an array of thermocouples and high-speed video images were used to characterise the size and distribution of the liquid droplets in the cascade.

The first part of this paper describes a series of hexane liquid releases in which the vapour cloud was free to travel away from the base of the cascade as it struck the ground. Measurements of the vapour temperatures from the experiments are compared to predictions from the CFD model and thermodynamic analysis. The second part investigates the effect of a bund wall on the vapour dispersion close to the base of the tank. A further set of experiments and CFD simulations were undertaken with a two-metre high vapour fence to examine the interactions of the vapour current with the bund wall. The presence of a bund resulted in the cascade entering into a layer of vapour and produced a vapour current with less tendency to mix and dilute.

1. Introduction

The falling liquid cascade from a tank overfilling release breaks up into filaments and spray droplets within a few metres from the tank rim. As the droplets fall, momentum is transferred to the surrounding air due to its entrainment into the spray. For volatile materials, which are the subject most of interest in the present study, this air entrainment lowers the vapour pressure around the droplets' surface and increases the mass transfer rate (i.e. increases the evaporation rate). The increase in vapour concentration in the falling cascade is also associated with a fall in temperature, due to the latent heat absorbed in transforming the liquid into gas. At the foot of the tank, the liquid droplets hit the ground forming a splash zone, from which the liquid runs away across the bund floor. The vapour that has been entrained into the falling spray also impinges onto the floor. The pattern of vapour flow from this impingement region can be complex, with some flow in lateral directions parallel to the tank walls and recirculation in the cavity between the spray and the tank wall. The bulk of the vapour current

flows outwards, away from the tank along the bund floor. Since the vapour current is cold and may contain high concentrations of hydrocarbons, in the case of gasoline spills, the vapour current will be dense and will tend to travel along the ground. If ambient conditions are relatively humid, the drop in vapour temperature may be sufficient for water to condense in the current and show itself as a visible mist. This phenomenon was observed in the Buncefield Incident, where CCTV footage showed a low-lying mist growing from the over-spilling tank in the minutes leading up to the explosion.

Figure 1 shows a schematic of the generation of a cold vapour current produced by a liquid cascade. Vapour created within the cascade is expelled at its base and travels outwards with an initial depth, *h* and velocity *U*. The current has a density, ρ_2 , differing from the ambient air density, ρ_1. This arrangement can be viewed as the continuous generation of a dense gravity current, a simplified analysis of which is presented by Fannelöp (1994).

Referring to Figure 1, the pressure at the front of the current is $1/2\ \rho_1 U^2$ and the reduced hydrostatic pressure under the current is $(\rho_2 - \rho_1)gh$. In the absence of friction, the relationship between these pressures is constant so that:

$$\frac{\rho_1 U^2}{2(\rho_2 - \rho_1)gh} = const \tag{1}$$

This expression is effectively the inverse of the Richardson number (*Ri*):

$$Ri = \left(\frac{\rho_2 - \rho_1}{\rho_1} \right) \frac{gh}{U^2} \tag{2}$$

The Richardson number expresses the ratio of the potential energy required to mix the fluids to the kinetic energy. An excess of kinetic energy results in the dense current mixing with the ambient air and diluting, and is characterised by a Richardson number much less than one. It follows that a flow with less tendency to mix should have a Richardson number much greater than one, i.e. should be dense, deep and slow moving, as observed in the Buncefield CCTV footage. This raises the question of how such a cloud can be created by a cascading liquid, which one might expect to be a fairly energetic process, given the quantity of liquid and a typical tank height of 10 m to 15 m.

Generally, hydrocarbon storage tanks are surrounded by some form of bund designed to contain liquid in the case of leaks or failure of the tank. As the vapour current moves outward, it will encounter the bund wall. The interaction of dense gravity currents with walls has been the subject of a great deal of research particularly in the field of dense gas dispersion where the mitigating effects of walls and fences are of interest. For example, Rottman *et al.* (1983) presented a two-dimensional analysis of the flow of a gravity current over a wall. In their analysis, the authors assumed that a steady state had been reached and they were principally interested in the relationship between the overall current depth and the wall height. They also carried out an unsteady analysis to determine the timescales involved in reaching this steady state from the initial moment the current strikes the wall. Similar analyses also involving two-dimensional shallow water theory were presented by Lane-Serff *et al.* (1995). A further study by Webber *et al*. (1994) examined a heavy gas cloud advected by the wind encountering a fence. Their model described a dilution process in which the dense cloud increased in size until it was sufficiently deep to surmount the fence.

In the current study, the primary interest is in the creation of a flammable vapour cloud, which is a function of a number of processes:

- The production rate of vapour by the liquid cascade
- Interaction of this vapour current with a bund wall
- The accumulation of vapour within the bund and its effect on the cascade
- The properties of the vapour overflowing the bund and dispersing into the surroundings.

Three-dimensional CFD modelling can provide a simultaneous description of all the above phenomena. In particular, it can be used to help understand the effects of the accumulation (or recirculation) of vapour within the bund. This is difficult to analyse using alternative methods, since it is inherently a transient process, with the liquid spilling into a vapour layer of increasing depth. Furthermore, CFD analysis can be used to explore aspects of vapour cloud generation not readily achieved experimentally. The mechanisms involved in the production of vapour clouds extends to other volatile materials, the general principles are discussed in Atkinson *et al* (2008).

2. CFD modelling of cascading liquids

The experimental apparatus, shown in Figure 2, consisted of a liquid storage tank set on top of a 10 m high tower with a wind girder situated at half height. An array of thermocouple masts was positioned on the concrete surface at the base of the tower. Measurements were also made of the liquid temperature in the spill chute and of the ambient temperature at several locations. Pressurised air was used to drive the liquid out of the storage tank and down the spill chute to a deflector plate. The deflector plate split the flow roughly in two, with half sliding down the front wall of the tower, striking the wind girder and spraying outward. The remaining half was projected out to fall the full 10 m. This behaviour corresponds to that observed in experiments undertaken with a mock-up of the Buncefield tank (Atkinson *et al* 2008). At the base of the cascade, the spilled liquid flowed into a drain, rather than accumulating in a pool. In the present work, the general-purpose CFD software, CFX 12.0 was used to model the release tower, liquid cascade and a section of the atmosphere.

For the computational model, the release tower was approximated as a rectangular box located on a flat surface as shown in Figure 3. The flow domain included a 50 × 80 × 30 m section of atmosphere to account for expected air movements due to the effects of entrainment. The extension of the domain in the longitudinal direction was necessary to allow a vapour current to travel uninhibited without reaching the boundary. Due to the deflector plate splitting the flow, the release point and wind girder flow were approximated as two individual releases. The upper release point was set to the width and height of the chute and the lower release point was given the same height and twice the width, based on observations from the experiments.

The present work adopts the same CFD methodology as used in the preliminary investigation by Gant & Atkinson (2007). The flow of air and vapour was modelled using an Eulerian approach which involves a computational mesh that is fixed in space through which the gases flow. Momentum, mass and energy conservation equations are solved in each mesh cell to find the velocity, temperature, pressure and concentration distributions. The spray of droplets was modelled using a Lagrangian approach in which the paths of discrete computational particles are tracked through the flow domain from their injection point until they hit a solid surface, escape the domain or evaporate completely. Each modelled fluid particle represents a large number of droplets with given mean size and transport properties.

The exchange of momentum, mass and heat between the Eulerian phase and Lagrangian particles is two-way. For momentum, particles falling through the air are subjected to drag

forces, and their trajectories can be affected by turbulent perturbations in the air. The air is also affected by the drag of the droplets and is entrained into the spray. Two-way coupling is important in determining evaporation rates, where the vapour concentration in the gas phase affects the rate of evaporation from the droplets and vice versa. Droplet evaporation leads to a temperature decrease which affects the saturation vapour pressure and hence the calculated evaporation rate. Coupling between the two phases is achieved by introducing source terms derived from the Lagrangian solution into the Eulerian transport equations. The overall CFD solution is obtained by iterating between the Eulerian and Lagrangian models.

A previous validation study for small-scale methanol sprays produced by pressurized releases from nozzles was undertaken by Gant *et al* (2007) and further validation of this approach can be found in Lim *et al* (2007). Details of the mathematical sub-models used for modelling evaporating sprays can be found in the software manuals (ANSYS, 2009).

An unstructured computational mesh was used with cells clustered near the release points, along the trajectory of the spray particles and close to the floor. Near the source, cells are typically a few centimetres across, whilst in the far field they grow to sides of around one metre or more. Tetrahedral cells are used in the majority of the flow domain and prism-shaped cells are used near the ground to increase the number of cells in the vertical direction and resolve the thin, dense, gravity current.

The open boundaries at the domain sides and top (representing the atmosphere) were set as entrainment boundaries, allowing the air velocities to freely develop whilst maintaining a set hydrostatic pressure. The 30 m domain height means that hydrostatic pressure has a significant effect on the density. Rather than specifying a uniform constant pressure, an analytical profile was used.

In the present work, the industry standard SST turbulence model has been used (Menter, 1994). At the start of the simulations, when the liquid first begins to cascade from the tank, it was assumed that the air velocity is zero everywhere. Very low but finite initial turbulence levels are also specified: an initial turbulence intensity of 5% (based on a reference velocity of 0.01m/s) and a ratio of the turbulent viscosity to the fluid viscosity of 10. A non-Boussinesq approach was adopted to model buoyancy effects, which is suitable for modelling a wide range of density variations. The effect of density variations on the flow turbulence was accounted for using standard buoyancy corrections in the turbulence transport equations, for details see ANSYS (2009).

To help understand the physical mechanisms of spray breakup and air entrainment in overtopping flows, preliminary experiments were undertaken involving releases of water. This enabled the release arrangement and instrumentation to be tested without the potential to produce a flammable vapour cloud. The preliminary runs with water were also used to validate the CFD modelling approach and provide a set of data against which to carry out sensitivity studies.

3. Unconfined hexane cascade

This section describes a set of simulations carried out using hexane as the spill material. The single component hydrocarbon, hexane, is used as a representative of petrol while avoiding the need to simulate a complex multi-component evaporation. The releases were at a flow rate similar to that observed at Buncefield in terms of mass released per unit length of spill chute. Simulations were performed using a 439,000 node mesh, with the following initial conditions:

- Total mass flow of hexane: 14.6 kg/s split evenly between the chute and wind girder
- Ambient temperature: 5ºC
- Hexane temperature: 4.2ºC
- Stable atmospheric conditions with nil wind
- Spill duration: 26 seconds

Primary breakup of the liquid sheet into droplets can be modelled using CFD. However, the CFD models have only been developed to model the breakup of liquid streams from devices such as high-pressure fuel injectors. Due to significant differences between such cases and the application considered here, in the present work the incoming liquid is assumed to be in droplet form at its point of release. Experiments carried out as part of the earlier Buncefield Investigation (MIIB, 2006a, 2006b, 2006c) suggested that hexane spills would form fairly uniformly-sized droplets of the order of 2 mm in diameter. Stills taken from high-speed video footage of more recent hexane spills undertaken as part of the present study gave similar results, with an average diameter of around 2 mm. Therefore as a starting point, simulations have been performed with a monodisperse spray of 2 mm droplets. Further runs were carried out with a range of hexane droplet sizes.

Figure 4 shows the temperature histories at thermocouple Masts 1 and 6 (corresponding to 3.2 m and 9.74 m respectively from the base of the tank wall) at the lowest measuring height. The temperature profiles exhibit a sharp drop followed by a recovery and then a steady-state period roughly halfway between the minimum and maximum temperature. The low initial temperatures arose from the droplets falling initially through fresh air, and therefore being free to evaporate to a large degree. By the time the vapour current reached Mast 6 at a distance of 9.74 m from the tank, it was diluted by ambient air and the temperature drop was approximately half the value at Mast 1. The hexane current took slightly less than 5 seconds to travel between Masts 1 and 6, with an average velocity of approximately 1.3 m/s.

Figure 5 compares the maximum temperature drop recorded at each mast in the experiments to the CFD predictions. The results show a rapid reduction in the temperature drop away from the tank wall. The shapes of the temperature profiles at the masts are largely governed by turbulent mixing and dilution of the cold current with ambient air. In addition to using 2 mm monosize hexane droplets, further simulations were carried out with 1 mm monosize droplets, a Rosin-Rammler size distribution and 5 mm droplets using the breakup model of Rietz & Diwakar (1986). The Rosin-Rammler size distribution was specified with a characteristic diameter of 2.21 mm and an exponent of 1.5, following the approach adopted by Gant & Atkinson (2007). Results for the different droplet sizes are presented alongside the 2 mm case in Figure 5. Both the 1 mm monosize and 2.21 mm Rosin-Rammler droplets resulted in slightly greater temperature drops than the experiment, whereas the 5 mm droplets produced only a small temperature drop. The 2 mm monosize droplets produced good agreement with the data for all but the first mast. The thermocouple trace at this position showed a rapid drop in temperature suggesting that in the experiments the thermocouple had been splashed with hexane liquid and was recording the evaporating liquid temperature rather than the vapour temperature.

The production of a vapour current from a liquid cascade involves two processes: a mechanical process in which air is drawn into the liquid cascade and mixed, and a thermodynamic process in which mass and energy are exchanged between the droplets and the air. A simple means to determine the volume flow rate of vapour produced by the cascade is to consider the temperature decrease in the vapour phase at the start and the end of a release. This approach was used to analyse the CFD simulations in which the vapour cloud remained within the computational domain for the duration of the calculation. The bulk temperature drop, ΔT_{bulk}, of the whole domain at the end of the release was calculated from:

$$\Delta T_{bulk} = \int_V \Delta T dV \tag{3}$$

where ΔT is the temperature drop of the gaseous phase at the end of the simulation for each cell and V is the volume of the domain. If it is assumed that the liquid and vapour reach equilibrium conditions in the core of the cascade, the temperature of the vapour as it leaves the cascade will be equal to the mean droplet temperature. The mean rate at which vapour is produced can therefore be approximated by dividing ΔT_{bulk} by the temperature drop from the initial ambient air temperature to the mean temperature of the droplets, and by the duration of the release (in seconds). Results of this analysis are summarised in Table 1. This simple approach ignores any convective heat transfer from the ground or the tank walls which are at a different temperature to the vapour current. Analysis of the experimental data suggests that this has a relatively minor effect on the cloud temperature, and the bulk of the temperature rise in the vapour current is due to mixing with ambient fresh air.

Table 1 Bulk properties at the end of the simulation

ΔT_{bulk} (m^3 °C)	1403.11
Initial vapour temperature (°C)	5
Final droplet temperature (°C)	-6.85
Cloud volume (m^3)	118.5
Spill duration (s)	26
Volume flow (m^3/s)	4.55
Initial concentration (mol/mol)	0.06

Although the CFD model predicts concentration, its value depends heavily on the location at which it is sampled. The benefit of the bulk analysis is that it also allows an estimate of the initial source concentration originating from the cascade. The calculated concentration of 0.06 mol/mol is slightly above the saturation concentration at the liquid temperature, indicating that the actual vapour temperature is slightly higher that the liquid temperature.

Figure 6 shows the gas phase temperature and vapour concentration as a fraction of the saturation vapour concentration (at the vapour temperature) on a plane through the centre of the cascade. The results are shown towards the end of the steady state period, after 26 seconds. The lowest vapour temperatures were produced at the base of the cascade at the point where the droplets struck the ground. On this central plane, the temperature of the vapour was generally a few degrees Celsius higher than the temperature of the droplets, and the lowest gas-phase temperatures were approximately -1.2 °C. On the central plane, the peak concentration was 78 % saturated and closer to 60 % in the lower regions of the cascade (Figure 6).

Predictions of the vapour current temperatures downstream from the spray zone for the 2 mm diameter monosize droplets were in good agreement with the experiments. This suggests that the model adequately predicted the overall entrainment of air and the exchanges of heat and mass. The general indication from both the model and the experiments is that thermal equilibrium was not fully reached by the time the droplets reached the base of the cascade. The impact of this on the calculation of the rate of air entrainment, described above, is fairly small as the heat capacity of air at 1.01 kJ/kg-K is approximately half that of the hexane liquid at 2.16 kJ/kg-K. Therefore, small changes in the assumed air temperature do not result in large changes in the entrainment rate and hence concentration predictions. The consequence of assuming thermal equilibrium is to underestimate the air entrainment rate, as a smaller drop in air temperature requires more mass to be mixed to provide the same quantity

of heat energy. In future experimental work, both liquid and vapour temperatures will be recorded to clearly establish the extent to which thermal equilibrium is reached.

Referring to Figure 1, average values of the density ratio $(\rho_2-\rho_1)/\rho_1$, and velocity (U) were calculated for the vapour current leaving the cascade, at a distance of 3 m from the wall. The depth (h) was set as the distance from the ground to an arbitrary concentration limit, in this case the Lower Flammability Limit (LFL). Inserting these values into Equation (1) results in a Richardson number of 0.01 indicating that the vapour current was dominated by kinetic effects and would tend to mix and dilute very rapidly. This is evident in the steep decrease in the temperature profiles shown in Figure 5.

4. Hexane cascade into a bund

The experiments and analysis presented so far indicate that the properties of the vapour current cause it to rapidly dilute by turbulent mixing with the ambient air. Evidence from Buncefield, however, suggested that it was possible to sustain a flammable vapour current for a distance of several hundred metres from the tank. When the cascade is surrounded by containment, such as a bund, the mixing and dilution process is changed significantly since the vapour cloud is no longer free to disperse. Instead, material emerging from the base of the cascade enters into a vapour rich region within the bund.

The spill rig was modified by the addition of a vapour fence intended to represent the bunding surrounding hydrocarbon storage tanks. The fence was set at a distance of 10 m from the base of the cascade and approximately 5 m either side of the cascade centre. Side panels were set at a distance of 5 m from the spill mid-plane to replicate the confining effects of adjacent spills on tanks with multiple release points. The fence was 2 m high constructed from plywood sheets attached to metal fencing. As with the unconfined cascade, spilled liquid was drained from the concrete base so that there was no pool accumulating within the fenced area. The same set of instrumentation was used, with some of the thermocouples in the array positioned outside the bund.

The modified computational geometry is shown in Figure 7. A 10 × 10 m walled enclosure around the spill area was created, leaving the geometry of the spill tower and domain size unchanged. The mesh size parameters were also unchanged, other than in the region of the bund wall. Due to the additional refinement near the bund wall, the total mesh size was increased to slightly over 1 million cells. The simulation was run with a 32 second spill period and carried on for a total of 60 seconds with the following settings:

- Mass flow of hexane: 11.7 kg/s total split uniformly between the chute and wind girder
- Ambient temperature: 11 ºC
- Hexane temperature: 10.3 ºC
- Stable atmospheric conditions with nil wind
- 2 mm monosize droplets
- Spill durations: 32 seconds and 120 seconds

The time histories of predicted temperatures are shown in Figure 8 for the lowest measuring height for Masts 1 and 6, again at 3.2 m and 9.74 m respectively from the spill rig wall. Mast 6 was situated just inside the bund wall. The results show similar trends to the unobstructed release up until 20 seconds, with a 3 °C temperature drop at Mast 1. After 20 seconds, the temperature at Mast 1 underwent a further drop of around 0.5 ºC. A fall in the temperature is also evident in the temperature profile at Mast 6. At the end of the spill period the temperature at Mast 1 increased abruptly by 1.5ºC, and further away from the tank wall at Mast 6 there was a corresponding more gradual increase in temperature.

A second simulation with the bund was carried out using the same boundary conditions as before but with the spill duration extended to two minutes. Figure 9 shows for the duration of the release the average predicted concentration and average temperature within the bund, and the vapour concentration at the single point just above the bund wall. The average concentration increased until approximately 80 seconds, where it reached a steady state value of 0.017 mol/mol. Assuming a maximum concentration within the cascade of 0.006 mol/mol (as calculated above), the average concentration represents a dilution factor of approximately 3.5. The mixture within the bund was less than the stoichiometric concentration for hexane of 0.022 mol/mol. In the initial stages of the simulation, the vapour flowing over the bund wall was slightly lower than the average concentration. However, once the steady state was reached, the vapour flowing over the top of the bund was slightly higher than the average concentration (0.019 mo/mol, compared to an average value of 0.017 mol/mol). Significant dilution of the vapour therefore occurred as the ambient air was drawn down into the bund by the cascade and this process was continuous.

The Richardson number of the vapour current leaving the bund was calculated using the approach described previously, at a position 3 m downstream of the bund. The resulting Richardson number of 0.15 indicates the vapour current leaving the bund had a significantly reduced tendency to mix with ambient air. For the unconfined case, the momentum of the vapour current was induced by the falling liquid over the 10 m height of the cascade. In contrast, the vapour flowing over the bund wall had available only 2 m of gravity head to drive the flow horizontally away from the bund. Although the material flowing away from the bund was marginally less dense than the unconfined case, the lower Richardson number was produced from the slower, deeper current.

5. Hexane cascade into a submerged bund

The previous section explored the influence of a bund on a hexane cascade. The vapour cloud produced by the cascade flowing into a bund was found to have a much lower tendency to dilute than the unconfined case. The bund eventually filled with vapour completely and overflowed in a relatively slow and deep layer.

In reality, this layer may not be maintained indefinitely to a uniform depth as it flows across the ground. Obstacles and topography can block or channel the dense vapour current and increase the initial depth of the layer. CCTV footage from the Buncefield Incident showed a low-level mist flowing across the ground adjacent to the overflowing tank shortly after the tank started overflowing. This is understood to be condensed water vapour that was carried by the current of dense petrol vapour. Over a period of around 20 minutes it was seen to increase to a depth of 3 to 4 metres in the area adjacent to the bund in which the release took place.

This section describes an exploratory set of simulations in which a 4 m high wall was placed around the perimeter of the computational domain. The aim of these simulations was to understand how increasing the depth of the layer affected the vapour production rate and the dispersion process. This arrangement could not easily be achieved using the experimental facility.

The computational geometry is shown in Figure 10. Details of the spill point and bund were unchanged from the previous simulations. Around the perimeter of the domain, a 4 m high wall was created replacing the lower sections of the open boundaries. In order to reduce computing costs, the overall domain width and length were reduced. The simulation was run with the same conditions as the previous bunded release. Average temperature and concentration within the bund were monitored and the simulation was continued until a steady state was reached. This required a spill duration of approximately 7 minutes and a total computing time of 7 days on a multi-processor fast desktop computer.

The average concentration and temperature within the bund, and the vapour concentration flowing over the top of the bund wall at a single point are shown for the duration of the release in Figure 11. The results show similar behaviour to the previous bunded spill with the average concentration increasing rapidly and then levelling off after around 90 seconds as a quasi-steady state is reached within the bund. The average concentration of vapour within the bund reached approximately 0.017 mol/mol, the same as that observed in the previous bunded spill.

After 100 seconds, the concentration began to rise further as vapour began to accumulate within the outer wall. Between 90 seconds and 120 seconds, the depth within the outer wall approached the height of the bund. The concentration and depth of material within the bund was therefore beginning to be influenced by the material accumulating in the outer wall. Later in the release, after 435 seconds, the mean gas concentrations and temperature showed signs of reaching a steady state. At this point, the concentration of the vapour flowing over the bund was the same as the average within the bund, at 0.024 mol/mol, slightly above the stoichiometric concentration of 0.022 mol/mol but less than that occurring within the core of the cascade where the concentrations were in the order of 0.033 mol/mol.

The fact that the average vapour concentrations in the bund continued to rise above the level reached in the simple bunded case indicate that some vapour is re-entrained into the cascade. However, the cascade continued to be fed by fresh air from above and the concentrations in the core of the cascade remained similar to an unconfined release.

Isosurfaces of the predicted vapour cloud at four concentration levels are shown in Figure 12 at the end of the simulation, once steady state conditions were established within the bund. The colour of the isosurfaces indicates the height from the ground, where the maximum height is set at 4 m corresponding to the height of the containment wall. The cloud depth as defined by the LFL at this stage reaches a uniform 4 m depth across much of the area. However, close to the tank, the LFL isosurface depth is lower, showing that the vapour is displaced by the ambient air that is entrained into the cascade. This effect is pronounced at the slightly higher 1.5 × LFL concentration. The vapour cloud at the stoichiometric concentration is confined to an area just beyond the bund walls. This is consistent with the concentration at the top of the bund walls being only slightly higher than stoichiometric (Figure 11). At 1.5 × stoichiometric, the isosurface is entirely limited to a small region surrounding the cascade. The influence of the bund and outer wall is therefore to cause re-entrainment of vapour into the vapour current flowing away from the cascade. The effect of this re-entrainment is an increase in concentration of the vapour flowing over the bund wall. However, fresh air continues to be drawn downwards by the liquid cascade. The dilution by this ambient air acts to limit the concentration that can ultimately be reached in the vapour cloud.

6. Conclusions

This paper describes a set of large-scale experiments and CFD simulations which have been carried as part of an ongoing study into the mechanisms behind the generation of vapour clouds from overfilling tank releases of liquid hexane. Use of the experiments to inform the simulations and vice-versa has enabled exploratory investigations using the model.

If it is assumed that there is thermodynamic equilibrium between the liquid and vapour in the cascade, the resulting concentration of hexane vapour leaving the cascade has been determined to be in the flammable range. However, there is very rapid dilution of the current as it leaves the cascade, and the Richardson number suggests that an unobstructed vapour current will tend to mix and dilute rapidly.

In order to investigate the effect of a bund wall on the vapour current, a 2 m high vapour fence was constructed around the base of the spill tower. CFD simulations of this arrangement were carried out. The vapour flowing over the bund wall has a much lower gravity head, driven by the height of the bund, rather than the cascade height. The simulations showed the concentration of this vapour to be slightly less than stoichiometric and less than half that emerging from the base of the cascade. This resulting Richardson number was higher than for the unconfined cascade, indicating a reduced tendency to mix and dilute.

In the Buncefield incident, it was observed that vapour accumulated in a layer of increasing depth. Eventually, this layer reached a depth such that the entire bund and part of the cascade were submerged. This effect could not be investigated experimentally but was modelled using CFD. A 4 m high wall was constructed round the domain and the simulation was run until the walled volume filled with vapour. The effect of a gradually deepening vapour layer was to increase the concentration of the material flowing over the bund wall as vapour was continually re-entrained into current leaving the base of the cascade. However, fresh air continued to be drawn downward by the cascade and this ultimately acted to limit maximum vapour concentration that could be achieved.

The simultaneous programme of experiments and simulation has enabled model validation and insight into vapour cloud generation from liquid cascades. The studies have provided a base for further work into the effects of release geometries.

7. Acknowledgements

This publication and the work it describes were funded by the Health and Safety Executive (HSE). Its contents, including any opinions and/or conclusions expressed, are those of the authors alone and do not necessarily reflect HSE policy.

8. References

ANSYS (2009) ANSYS CFX-12 User Guide. ANSYS, Inc., Canonsburg, Pennsylvania, USA

Atkinson, G., Gant, S. E., Painter, D., Shirvill, L. C. and Ungut, A., 2008, Liquid dispersal and vapour production during overfilling incidents. Proc. IChemE Hazards XX Symposium & Workshop, Manchester, UK.

Fannelöp, T. K., 1994, Fluid Mechanics for Industrial Safety and Environmental Protection, Industrial safety series 3, Elsevier.

Gant, S. E. and Atkinson, G. T., 2007, Flammable vapour cloud risks from tank overfilling incidents. Health & Safety Laboratory Report MSU/2007/03 (currently only in draft form).

Gant, S. E., Heather, A. J. and Kelsey, A., 2007, CFD modelling of evaporating hydrocarbon sprays. Health & Safety Laboratory Report CM/07/04.

Lane-Serff, G. F., Beal, L. M. and Hadfield, T., D., 1995, Gravity current flow over obstacles, Journal of Fluid Mechanics, 292, Pages 39-53.

Lim, E. W. C., Koh, S. H., Lim, L., K., Ore, S., H., Tay, B., K., Ma, Y. and Wang, C., 2008, Experimental and computational studies of liquid aerosol evaporation, Journal of Aerosol Science, Volume 39, Issue 7, Pages 618-634.

Menter, F. R., 1994, Two-equation eddy-viscosity turbulence models for engineering applications. AIAA Journal, 32, pages 1598-1605.

MIIB, 2006a, Buncefield Investigation Progress Report. Major Incident Investigation Board (MIIB).

MIIB, 2006b, Buncefield Investigation Second Progress Report. Major Incident Investigation Board (MIIB).

MIIB, 2006c, Buncefield Investigation Third Progress Report. Major Incident Investigation Board (MIIB).

Reitz, R. D. and Diwakar, R., 1986, Effect of drop breakup on fuel sprays. SAE Technical Paper Series, No. 860469.

Rottman, J. W. and Simpson, J. E., 1983, Gravity currents produced by instantaneous releases of a heavy fluid in a rectangular channel, Journal of Fluid Mechanics, Volume 135, pages 95-110

Webber, D. M., Jones, S. J. Martin, D. Tickle, G., A and Wren, T, 1994, Complex Features in Dense Gas Dispersion Modelling, UKAEA Report AEA/CS/FLADIS/1994 (Volumes I and II)

Figures

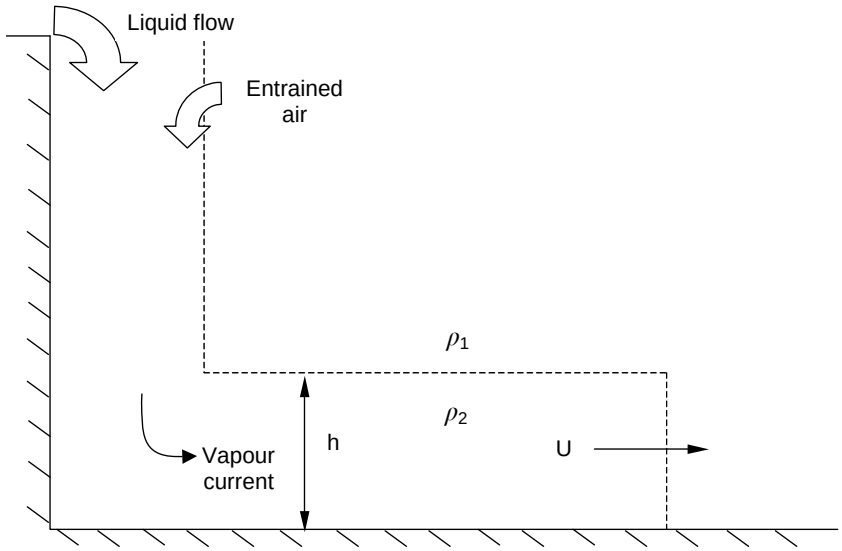

Figure 1 The properties of a vapour current produced by a liquid cascade

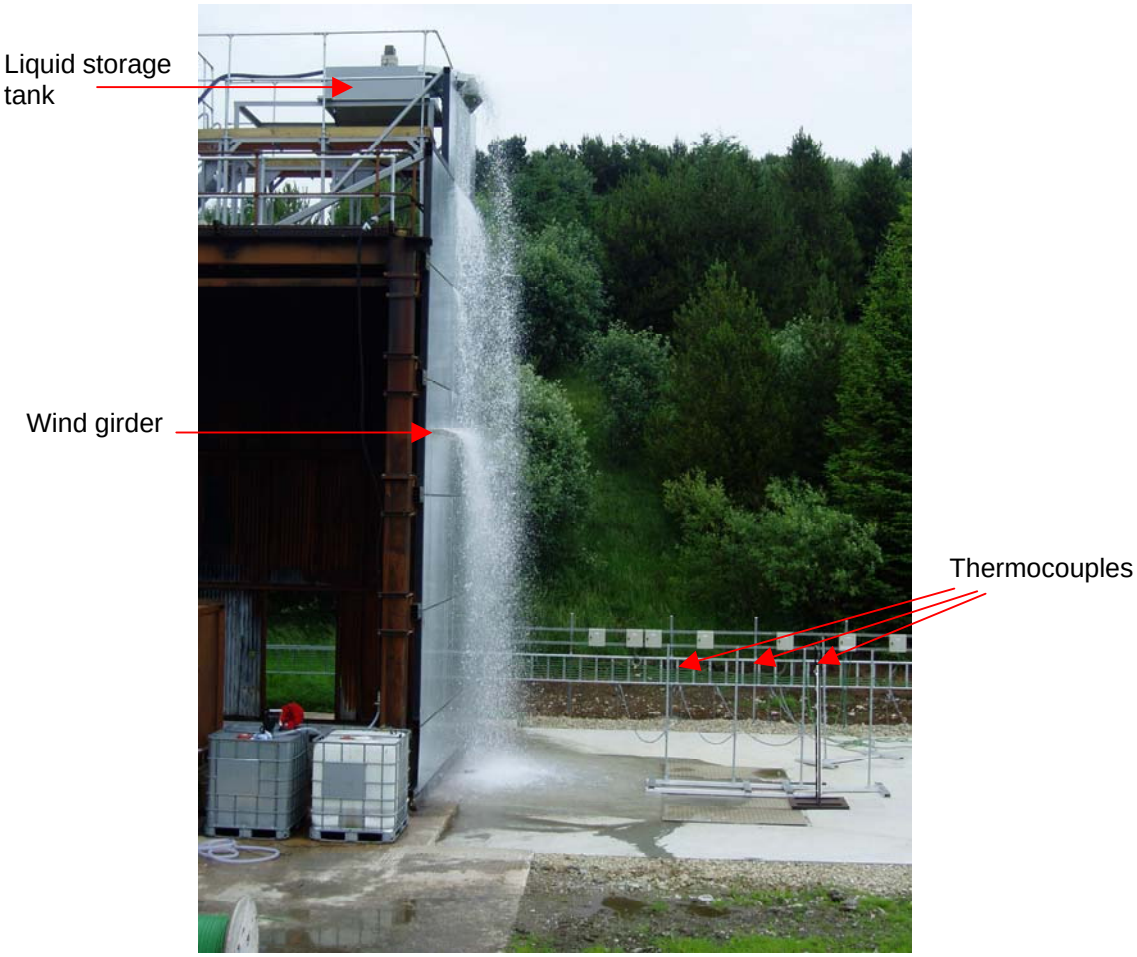

Figure 2 The spill rig showing the release tower and thermocouple array

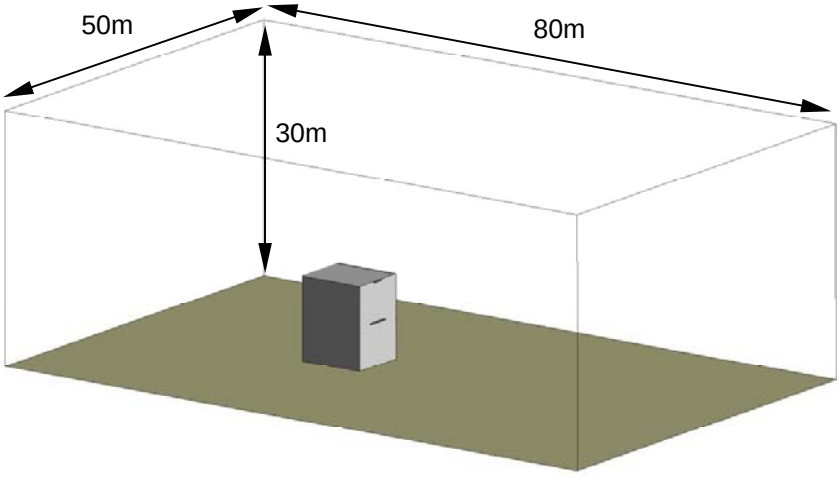

Figure 3 Computational geometry

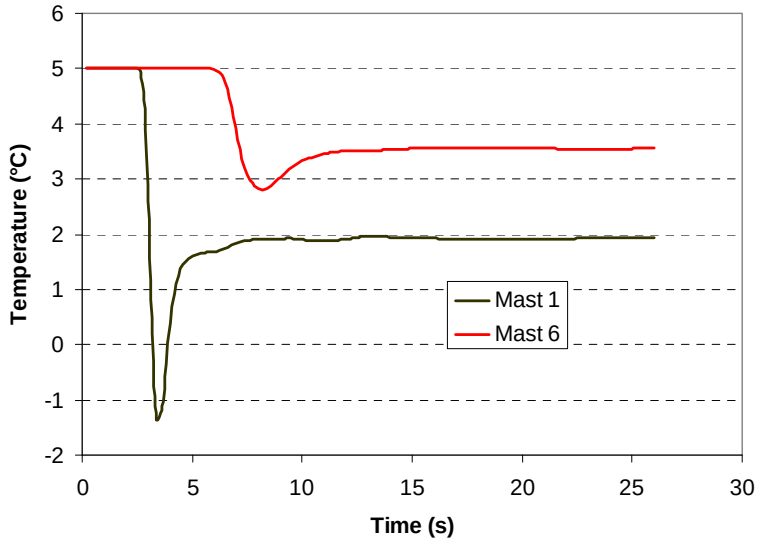

Figure 4 Predicted temperatures at Masts 1 and 6

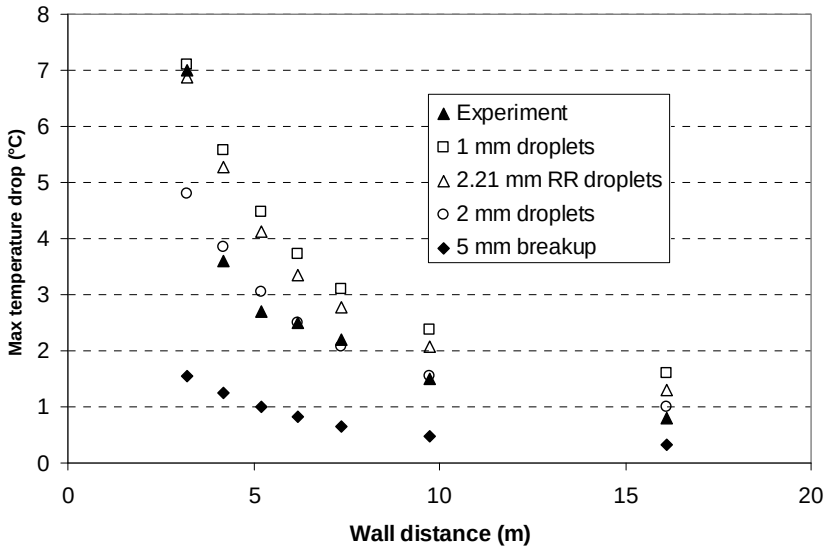

Figure 5 Vapour temperatures for the hexane release with different modelled droplet sizes

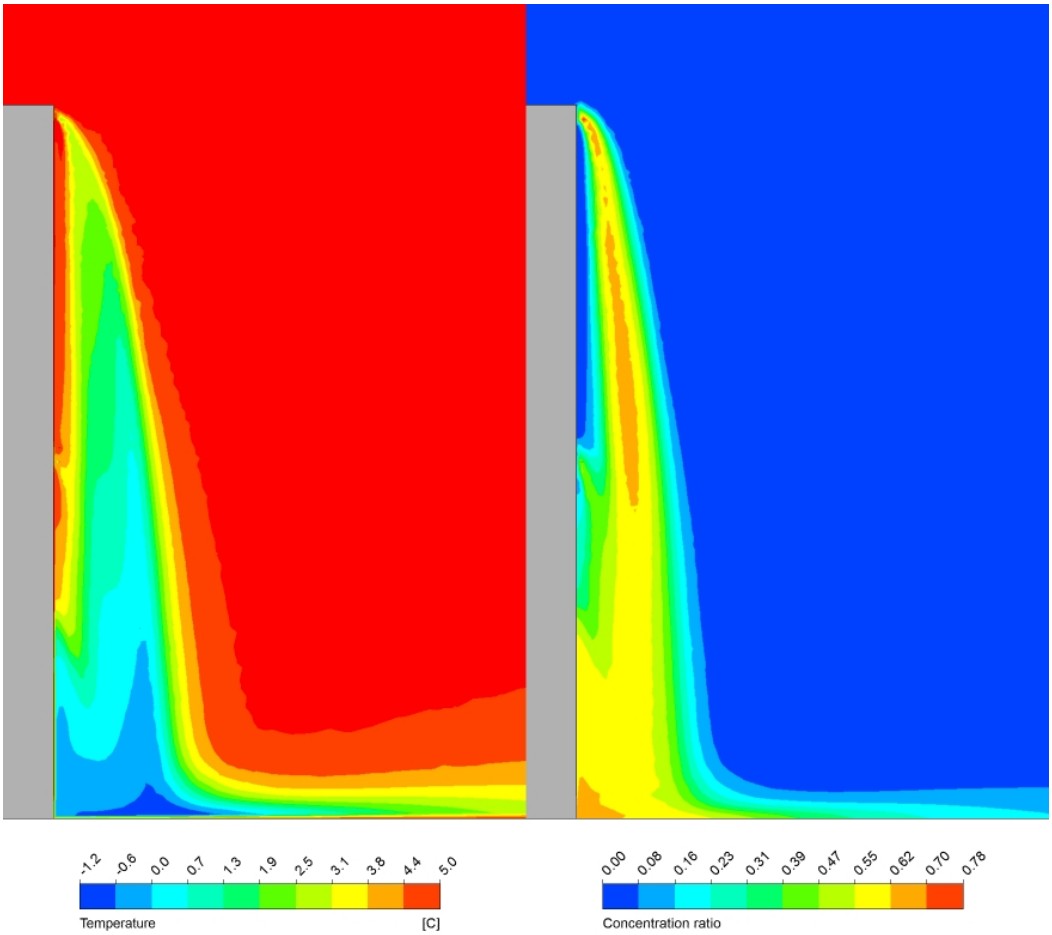

Figure 6 Predicted gas phase temperature and concentration, shown in terms of the saturation fraction.

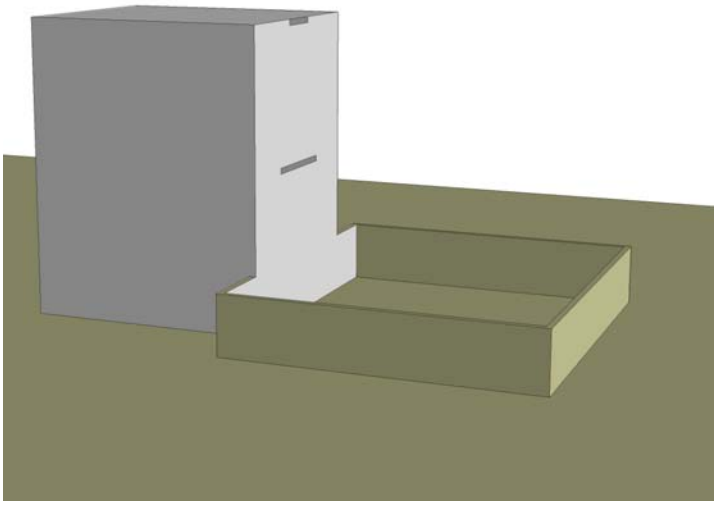

Figure 7 Computational geometry with bund

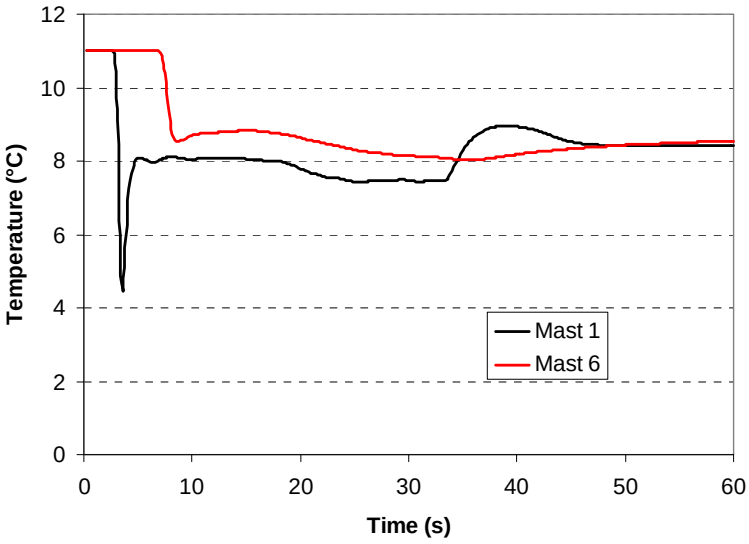

Figure 8 Predicted temperatures at Masts 1 and 6

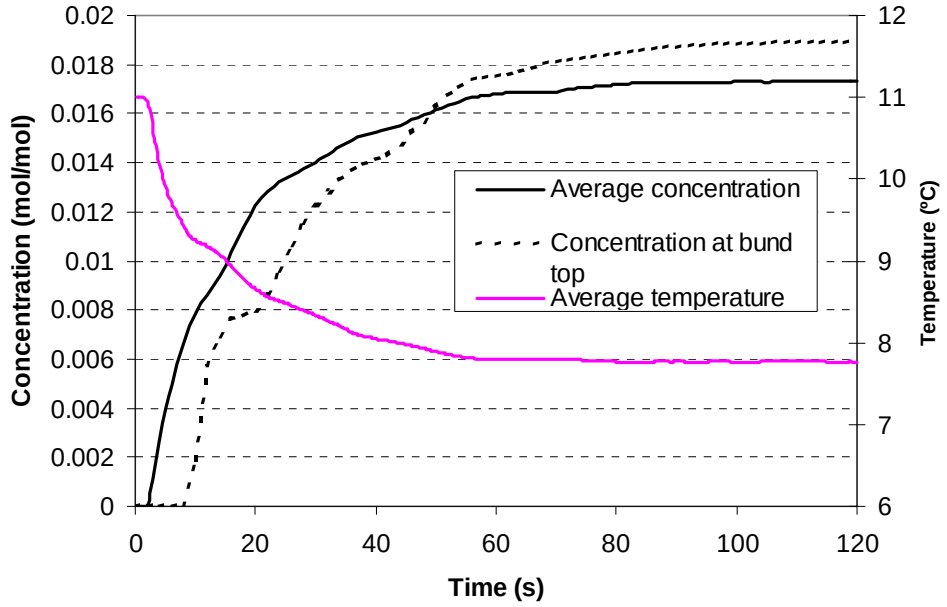

Figure 9 Predicted average concentration and temperature within the bund for a continuous release of 120 seconds. The concentration of material flowing over the bund top at a single point is shown by the dashed line.

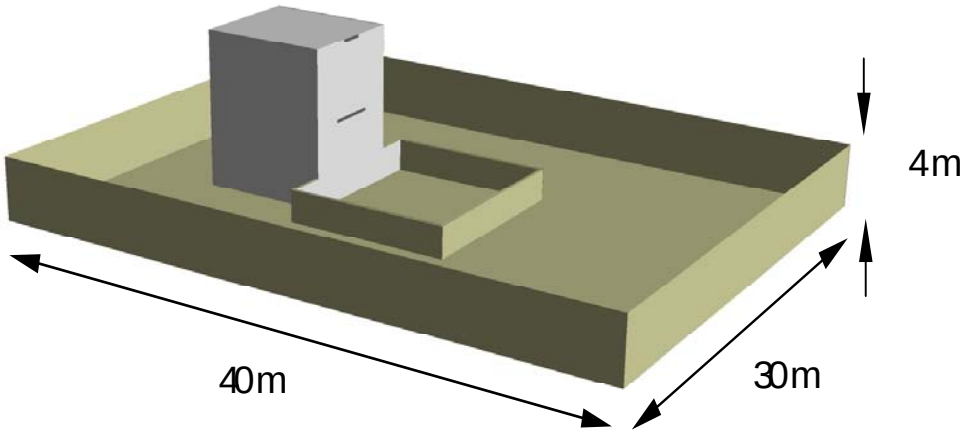

Figure 10 Computational geometry with bund and 4 m vapour barrier

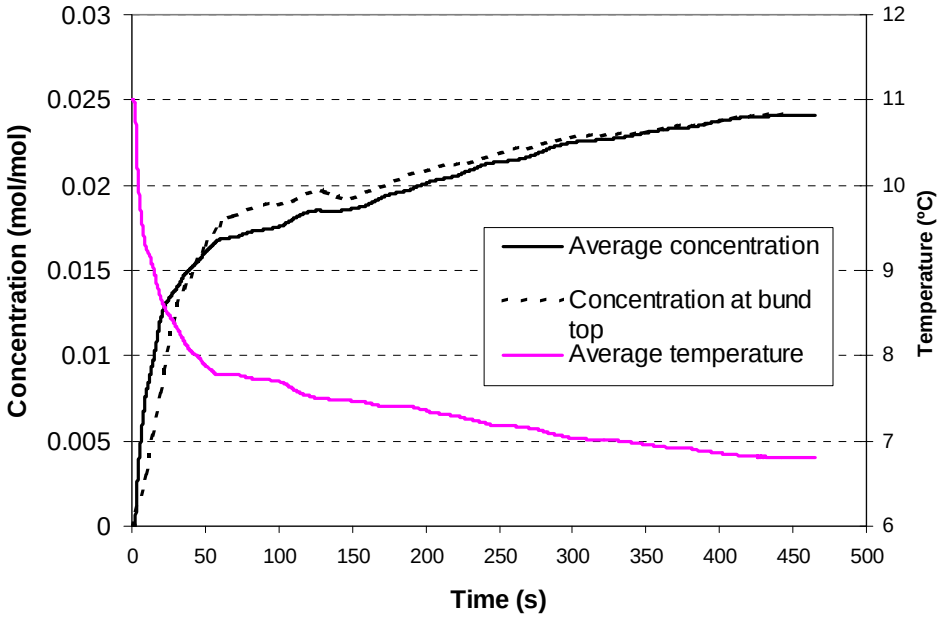

Figure 11 Predicted average concentration and temperature within the bund. The concentration of material flowing over the bund top at a single point is shown by the dashed line

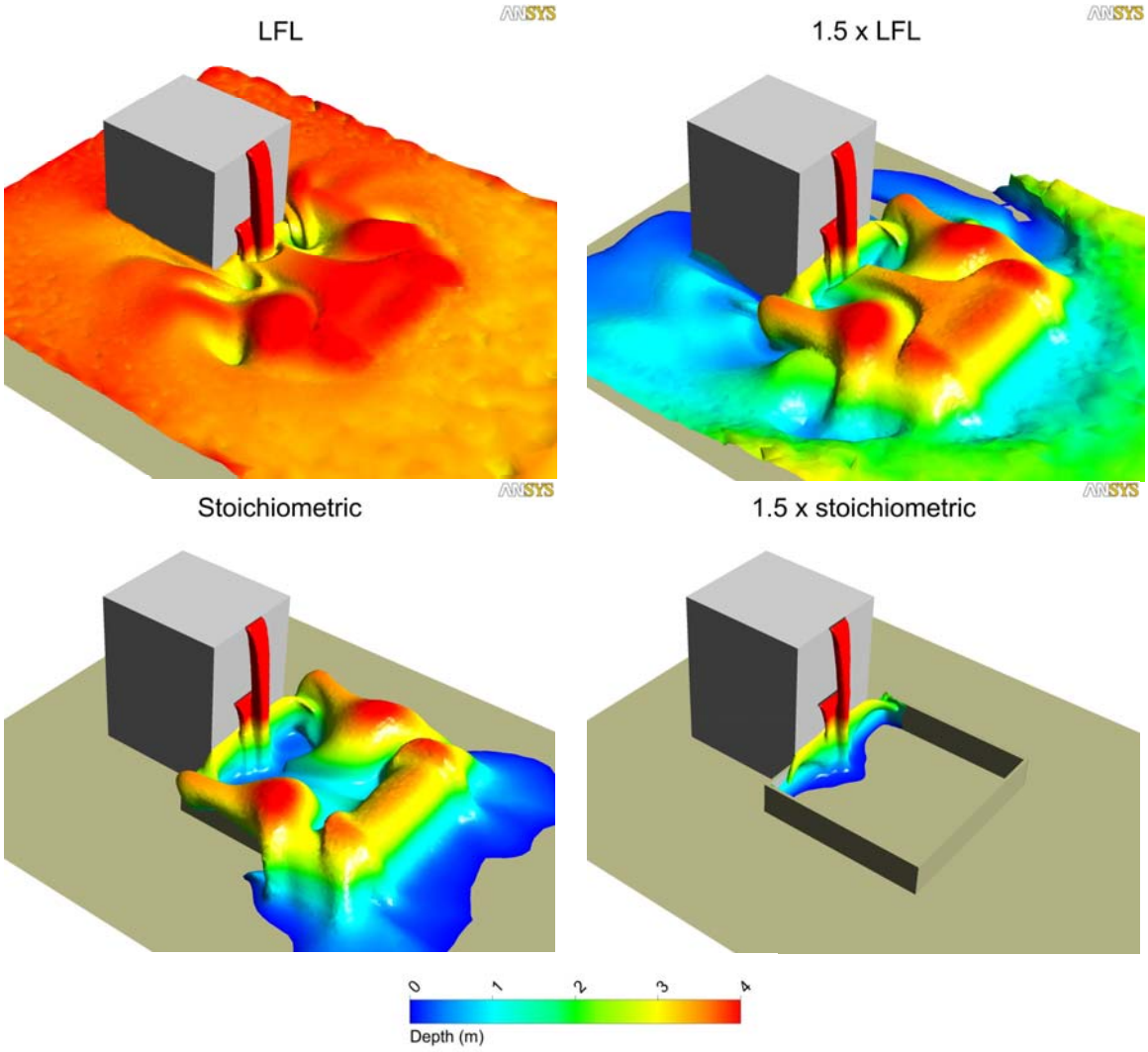

Figure 12 Isosurfaces of the vapour cloud at increasing concentrations. The isosurfaces are coloured with height from the ground with a maximum height of 4 m.